GSA Data Repository 2019010
Drignon, M.J., Nielsen, R.L., Tepley F.J., III, and J. Bodnar, R.J.,, 2018, Upper mantle origin of plagioclase megacrysts from plagioclase-ultraphyric mid-oceanic ridge basalt: Geology, https://doi.org/10.1130/G45542.1

APPENDIX 1. METHODOLOGY

Homogenization Experiments and Sample Preparation for Volatile Analysis

Essentially all plagioclase-hosted MI have undergone significant post entrapment crystallization and contain one or more vapor bubbles. The reasons for the extent of post entrapment crystallization may be linked to two factors: (1) the host magmas are often significantly less primitive than the melts from which the megacrysts formed; (2) the phase equilibria of plagioclase results in twice the amount of crystallization per degree as for olivine (Kohut and Nielsen 2003). Therefore, reconstruction of the composition of the initial composition of the melt requires homogenization (Fig. DR1). Homogenization experiments were carried out using a 1-atm vertical furnace at Oregon State University by suspending 3 to 6 crystals in a platinum boat within the furnace at the entrapment temperature of 1230°C. That temperature was determined based on trial and error, was constrained by the olivine plagioclase cotectic and was confirmed using a heating stage (Sinton et al., 1993; Nielsen et al., 1995; Kohut and Nielsen, 2003; Nielsen, 2011). At the end of a run the samples were quenched in water. To test plagioclase crystals are reliable pressure vessels, samples were homogenized for 30 minutes, which is a typical time for homogenization experiment, and for to 4 days. The assumption was that the total reconstructed CO_2 concentration of the MI should not change as a function of experimental run time. Once homogenized for post entrapment crystallization, the plagioclase crystals were polished individually by fixing them on a round glass slide with crystal bond. Coarse silica grids of 600 and 1200 μm were used to remove the crystal bond from the surface of the plagioclase crystals and expose the melt inclusions. Once the MI were exposed, alumina powders of 5, 3 and 0.1 μm were used to finish polishing and remove any silica grid left on the crystals. The crystal bond was then dissolved in acetone, followed by a cleaning in a sonic bath with an alcoholic solution for 1h. The plagioclase crystals were then pressed flat into wells filled with indium drilled into 1-inch aluminum

mounts. Once mounted in indium, the MI were evaluated for the following: cracks in or around the melt inclusions; any irregular melt inclusion shapes; the presence of daughter crystals; and/or the presence of unusually large (>10 % by volume of inclusion) vapor bubbles. Any MI meeting any of those criteria (~20% of total) was discarded from further analyses (Moore et al., 2015).

Raman Analysis: CO_2 in the Vapor Bubbles

CO_2 analysis within the vapor bubbles of MI were performed at Virginia Tech (VT) on a JY Horiba LabRam HR (800 mm) Raman spectrometer. The instrument was set up to work with a 514-nm argon laser, a confocal hole diameter of 400 μm, a slit width of 150 μm, and a grating of 1800 mm-1. A synthetic fluid inclusion was used as a standard to test for the reproducibility of the Fermi-diad determination (Sterner and Bodnar 1984). Each analysis was performed with three 45-second scans that were averaged. The LabSpec software was used to apply baseline correction on each analysis and make the peak fittings on the Fermi-diad by applying a Gaussian fitting. From the peak fitting results, the values of peak splitting were determined, and the CO_2 densities calculated following the calibration curve = -36.42(0.31) + 0.355 (0.01) CO_2 (Lamadrid et al., 2017). After determining the CO_2 densities, the CO_2 concentrations of the vapor bubbles, and error analyses, were performed following Moore et al. (2015). It should be noted that no CO_2 was detected in the vapor bubbles of a melt inclusion homogenized for 4 days (sample: 4_1_3). Consequently, only the volatile concentrations obtained by SIMS analyses with their associated errors are displayed.

It is important to note that S was present as SO_2 within some of the vapor bubbles after the 30-minute runs based on the presence of a Raman peak at ~1151 cm^{-1}. However, we did not attempt to quantify the amount of S contained in the vapor bubbles because the Raman spectral features of SO_2 have not been calibrated as a function of pressure or density.

SIMS Analysis: CO_2 and Other Volatiles in the Glass of Melt Inclusions

Volatile analyses (H_2O, CO_2, S, F and Cl) of the melt inclusions' glasses were performed at Woods Hole Oceanographic Institution (WHOI) on a CAMECA IMS 1280, a secondary ion mass spectrometer (SIMS). These melt inclusions were the same as the ones analyzed on the Raman at VT. A synthetic forsterite with SiO_2 of 42 wt.% (SynFo) and a basaltic glass (519-4-1) of similar CO_2 concentration as expected from the MI, pressed into indium mounts, were regularly used as standards to check for instrumental drift. The mounts were cleaned, then dried in an oven at 65°C for > 2h. Once dry, the mounts were gold-coated and placed in a vacuum oven at 110°C for several hours until placed into the instrument to let them outgas. Next, each mount sat in the SIMS airlock for at least 8h at $5.0E^{-9}$ torr for further outgassing before being introduced to the sample chamber at pressures < 3.0E-9 torr. $^{133}Cs+$ was used as the primary beam (1nA, 10 micron). The primary beam focused on a 20 μm/20 μm area, and the aperture was set up to analyze a 7.5 μm/ 7.5 μm area. Each spot was pre-sputtered for 3 min, then each mass (^{12}C, $^{16}O\ ^{1}H$, ^{19}H, ^{30}Si, ^{32}S, ^{35}Cl) was analyzed over 5 cycles for a total analysis time of 9 min. Mass interferences of ^{17}O from $^{16}O\ ^{1}H$, and $^{29}Si\ ^{1}H$, from ^{30}Si were resolved by entrance and exit slit widths yielding a mass resolving power >6000. As the MI had higher S and CO_2 concentrations, the spot position on the sample was checked by verifying the intensity of the ^{32}S and ^{12}C. Nine standards glasses with different H_2O and CO_2 concentrations were used to make the calibration curves on $^{12}C/^{30}Si$, $^{16}O^{1}H/^{30}Si$, $^{19}F/^{30}Si$, $^{32}S/^{30}Si$, and $^{35}Cl/^{30}Si$. During analyses, the stability of the signal was carefully monitored for any sign of sample contamination. The detection limits were the following: 30 ppm for CO_2; 0.02 wt.% for H_2O; 1.2 ppm for S; 1 ppm for Cl; and 1.8 ppm for F.

MI were determined to be "un-breached" or intact based on their S concentration. Any MI with S concentration at, or below 90 ppm was considered breached and not further considered for this study. Indeed, MORB melts are supposed to be saturated with S (Wallace and

Carmichael, 1992). Based on their S concentrations, only 2 MI were considered breached, one for each run time (TABLE DR1).

The two main sources of error were investigated to perform the error analysis. A bootstrap regression was performed on the calibration to estimate the calibration errors. A time-based background analysis was used to check for any analytical drift with time on H_2O. Drift, if present, was corrected and applied to the data. As a result, the volatile concentrations presented are calculated based on the corrected calibration curves. The errors shown as 2 were established by propagation analysis of the corrected calibration curves and corrected volatile concentration for each sample.

Once the CO_2 concentrations were determined from both the vapor bubbles and the melt of a single melt inclusion, total CO_2 reconstruction and errors associated were calculated as per Moore et al. (2015). Following Moore et al. (2015), the first source of error is in the 2-D measurement of the long and short axes of both the melt inclusions and vapor bubbles. These errors are estimated to be 0.5 μm for any 2-D measurements. Errors on 2-D measurements are then propagated on the estimation of the volumes of both vapor bubbles and melt inclusions, which themselves are propagated with SIMS and Raman analytical errors to give the final errors on the CO_2 concentrations as + and – for one datapoint (TABLE DR1).

Pressures were calculated using VolatileCalc2.0 (Newman and Lowenstern, 2002) using SiO_2 = 49 wt.%, T = 1230°C, as well as the H_2O analyzed from the melt inclusions' glass, and the total CO_2 reconstructed from vapor bubble and glass analyses. Although more recent models are available to interpret H_2O-CO_2 data from MI (Papale et al., 2006; Shishkina et al., 2014; Ghiorso and Gualda, 2015), the models are all based on the same fundamental experimental data and differences between models are insignificant for the purposes of this study.

All data can be found in TABLE DR1.

T-test: Statistics comparing the volatile and pressure estimates of the 30-min and 4-day runs

T-tests were calculated using the online GraphPad software to compare the volatile and pressure estimates obtained for the 30-minute and 4-day runs. We used the unpaired t-test option that compares two datasets of the same parameter. The aim was to understand whether the differences observed were statistically significant. The t-tests compare one variable at a time for the two experimental run times. All the data obtained for CO_2 in the glass, H_2O in the glass, total CO_2 reconstructed, pressures, and $\%CO_2$ present within the vapor bubbles were computed for these t-tests (TABLE DR2). The outcome of a t-test is the P-value. The P value is comprised between 0 and 1 and represent the probability for one variable represented in two populations for the null hypothesis to be true. In other words, the closest P is to 0, the more likely the two populations sharing that same variable are statistically distinct. Note that for $\%CO_2$, we discarded 4_1_3 which has no CO_2 within its vapor bubble.

APPENDIX 2. MG# OF THE MELT INCLUSIONS AND POST ENTRAPMENT CRYSTALLIZATION CALCULATIONS

To assess the primitiveness of the MI, the Mg# of MI held at 1230°C for both 30 minutes and 4 days were calculated. Mg# was calculated assuming

$Fe^{2+} = 0.9 \times FeO_{total,}$ (Equation 1)

so that $Mg\# = 100x(Mg/Mg+Fe^{2+})$ in atomic proportions (Equation 2; Fig. DR2; TABLE DR3).

This data was gathered on different set of MI than those presented in this review, but they are nevertheless from the same sample (A91-1R). Due to the small size of the MI (20-30 μm), it was impossible to perform both chemical and volatile analyses without C contamination from coating for EMP analyses. The calculated Mg# are near-primitive melt compositions to both

experimental run times (Michael and Chase, 1987; Michael and Graham, 2015; Saal et al., 2002). For each dataset, the maximum Mg# was assumed to be unaffected by post-entrapment crystallization, therefore was used as the basis for the calculation of a linear regression. Based on the Mg#, the F parameter was calculated so that

$$F = Mg\#/Mg\#_{\text{highest of the dataset}} \quad \text{(Equation 3)}$$

From the F parameter, the linear regression was calculated using

$$\%\text{crystallization} = 100-(F*100) \quad \text{(Equation 4)}$$

The Mg# of the 30-minute runs show near-primary compositions compared to the host lavas. MI heated for 30 minutes have a Mg# of 67.53±2.48 (2). The Mg# are higher in the 4-day runs due to diffusive re-equilibration with their host (Fig. DR2; TABLE DR3). The linear regressions indicate that the MI have seen <10% of fractional crystallization post-homogenization experiment compared to that representing the most primitive member of the array of melts. The linear regressions also show that our MI are near to being primary in nature (Michael and Graham., 2015; TABLE DR3; Fig. DR2). In addition, the high Mg# of our samples suggest that $Fo_{88.5}$ olivine would be in equilibrium with those melts (Hughes, 1982). We suggest that these olivine crystals are found within the same troctolite cumulates that our plagioclase crystals originated from, but that their high density prevents them from being erupted with the plagioclase megacrysts.

The 4-day runs exhibit more primitive values and fit on a different linear regression than the 30-minute runs (Fig. DR2; TABLE DR3). This difference is likely due to re-equilibration processes occurring with increasing run times, where Mg from the plagioclase-hosts diffuses within the MI. Therefore, the 4-day data represents anomalously primitive melts, as the original chemistry of the MI was irreversibly modified by experimentation.

REFERENCES CITED

Ghiorso, M. S., and Gualda, G. A., 2015, An H2O–CO2 mixed fluid saturation model compatible with rhyolite-MELTS: Contributions to Mineralogy and Petrology, v.169, p.53, https://doi.org/10.1007/s00410-015-1141-8.

Kohut, E.J., and Nielsen, R.L., 2003, Low-pressure phase equilibria of anhydrous anorthite bearing mafic magmas: Geochemistry, Geophysical Geosystems, v.4, p. 1057, https://doi.org/10.1029/2002GC000451.

Lamadrid, H. M., Moore, L. R., Moncada, D., Rimstidt, J. D., Burruss, R. C., and Bodnar, R. J., 2017, Reassessment of the Raman CO_2 densimeter: Chemical Geology, v.450, p.210-222, https://doi.org/10.1016/j.chemgeo.2016.12.034.

Michael, P.J., and Chase, R.L., 1987, The influence of primary magma composition, H_2O and pressure on mid-ocean ridge basalt differentiation. Contributions to Mineralogy and Petrology, v.96, i.2, p.245-263.

Michael, P.J., and Graham, D.W., 2015, The behavior and concentration of CO_2 in the suboceanic mantle: inferences from undegassed ocean ridge and ocean island basalts: Lithos, v. 236-237, p. 338-351, https://doi.org/10.1016/j.lithos.2015.08.020.

Moore, R.L., Gazel, E., Tuohy, R, Lloyd, A.S., Esposito, R., Steele-MacInnis, M., Hauri, E.H., Wallace, P.J., Plank, T., and Bodnar, R.J., 2015, Bubbles matter: an assessment of the contribution of vapor bubbles to melt inclusion volatile budgets: The American Mineralogists, v.100, p.806-823. https://doi.org/10.2138/am-2015-5036.

Newman, S., and Lowenstern, J.B., 2002, VolatileCalc: a silicate melt-H_2O-CO_2 solution model written in Visual Basic Excel: Computers & Geosciences, v.2, p.597-604, https://doi.org/10.1016/S0098-3004(01)00081-4.

Nielsen, R.L., Crum, J., Bourgeois, R., Hascall, K., Forsythe, L.M., Fisk, M.R., and Christie, D.M., 1995, Melt inclusions in high-An plagioclase from the Gorda Ridge: an example

of the local diversity of MORB parent magmas: Contributions to Mineralogy and Petrology, v.122, p.34-50.

Nielsen, Roger L., 2011, The effects of re□homogenization on plagioclase hosted melt inclusions: Geochemistry, Geophysics, Geosystems, v.12, no.10, https://doi.org/10.1029/2011GC003822.

Papale, P., Moretti, R., and Barbato, D., 2006, The compositional dependence of the saturation surface of H2O+ CO2 fluids in silicate melts: Chemical Geology, v. 229, no. 1-3, p. 78-95, https://doi.org/10.1016/j.chemgeo.2006.01.013.

Saal, A. E., Hauri, E. H., Langmuir, C. H., and Perfit, M. R., 2002, Vapour undersaturation in primitive mid-ocean-ridge basalt and the volatile concentration of Earth's upper mantle. Nature, v. 419, p.451-455.

Shishkina, T.A., Botcharnikov, R.E., Holtz, F., Almeev, R.R., Jazwa, A.M., Jakubiak, A.A., 2014, Compositional and pressure effects on the solubility of H2O and CO2 in mafic melts: Chemical Geology, v.388, p.112-129, https://doi.org/10.1016j/chemgeo/2014.09.001.

Sinton, C. W., Christie, D. M., Coombs, V. L., Nielsen, R. L., and Fisk, M. R., 1993, Near-primary melt inclusions in anorthite phenocrysts from the Galapagos Platform: Earth and Planetary Science Letters, v. 119, no.4, p.527-537.

Sterner, S.M., and Bodnar, R.J., 1984, Synthetic fluid inclusions in natural quartz I. Compositional types synthesized and applications to experimental geochemistry: Geochimica et Cosmochimica Acta, v. 48, p.2659–2668.

Wallace, P.J., and Carmichael, I.S.E.,1994, Sulfur speciation in submarine basaltic glasses as determined by measurements of S Ka X-ray wavelength shifts: The American Mineralogist, v.79, p.161-167.

FIGURE CAPTIONS

Figure DR1. A) BSE images of MI prior to homogenization experiment showing post entrapment crystallization in grey and vapor bubbles in black. B) BSE image post homogenization showing MI free of post entrapment crystallization, but with vapor bubbles.

TABLE DR1. Details of the run times, sample names, CO_2 concentrations in both glass and vapor bubble of melt inclusions, as well as the total CO_2 concentrations. The top of the table shows the data for MI that were considered for this study. The lower part of the table shows the dissolved volatile concentrations of the two melt inclusions that breached and were discarded. The vapor bubble volumes are shown in column 6 with their lower and upper volume estimates (based on error propagation). The H_2O, SO_2, Cl, and F concentrations of the melt inclusion glasses are also shown. The calculated pressures from VolatileCalc 2.0 are displayed (Newman and Lowenstern, 2002), as well as the depths calculated by multiplying by 3 the pressure estimates. The errors on the volatile concentrations, the pressures and depths are shown as well.

TABLE DR2. Results of the t-tests performed to prove whether two groups of one variable are statistically different. The P values constitute the outcome of the t-test. Results from CO_2 (glass), H_2O (glass), Total CO_2, Pressures and % CO_2 in vapor bubbles are statistically compared in between the 30-minute and 4-day runs.

Figure DR2. Graph showing the results of the linear regression showing Mg# versus % crystallization for MI homogenized for both 30 minutes and 4 days.

TABLE DR3. Mg#, MgO (wt.%), FeO (wt.%), parameter F, and % crystallization calculation assessed by linear regression for MI homogenized for both 30 minutes and 4 days. Means and

219 standard deviations (2) are also shown.

220

Before homogenization experiment

After homogenization experiment

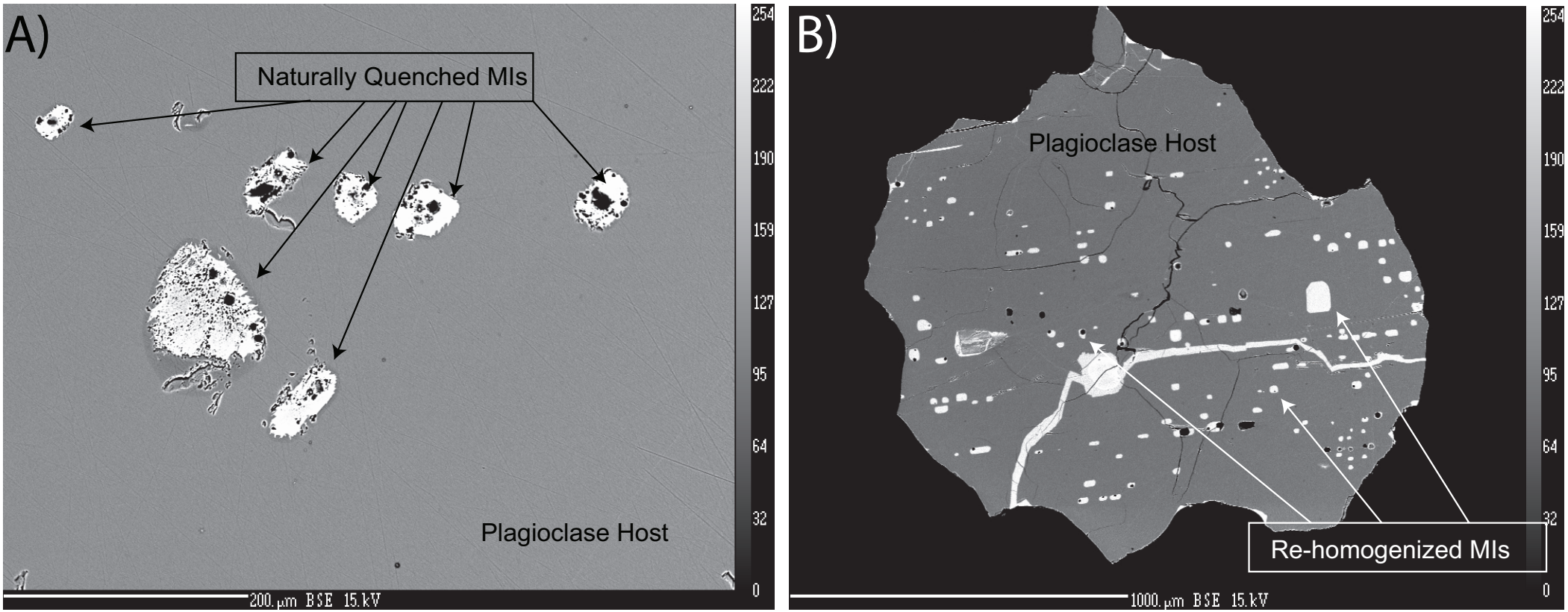

Fig. DR1

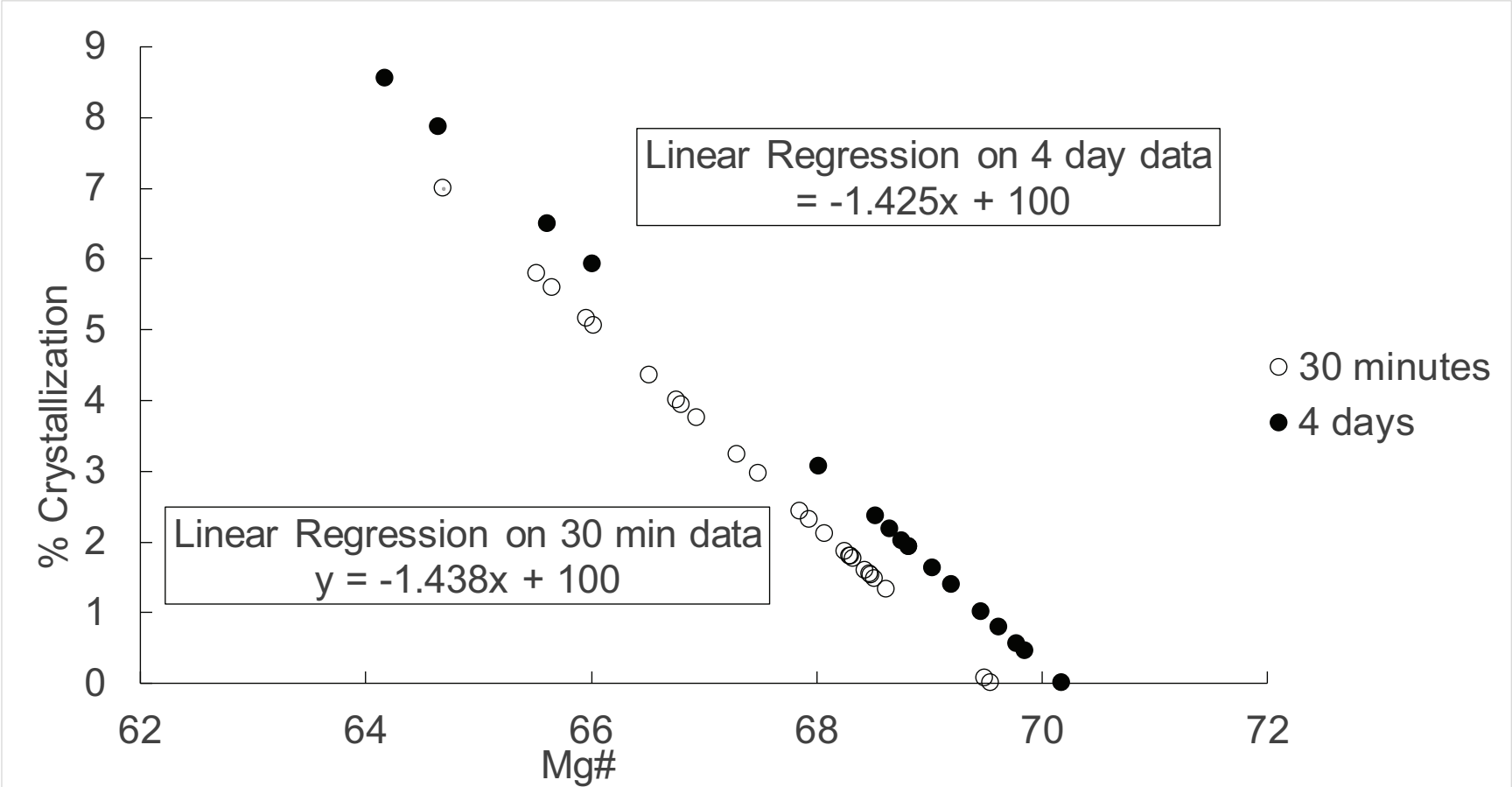
Linear Regression on 4 day data
= -1.425x + 100
Linear Regression on 30 min data
y = -1.438x + 100
30 minutes
4 days
% Crystallization
Mg#
0
1
2
3
4
5
6
7
8
9
62
64
66
68
70
72

TABLE DR1. Details of the volatile content and pressure and depth of entrapment for each MI analyzed

TABLE DR2. Unpaired t-test results

	P value	Statistically different?
CO_2 in glass	0.70	No
H_2O in glass	0.05	No
Total CO_2	0.13	No
Pressures	0.13	No
%CO_2 in vapor bubble	0.006	Yes

TABLE DR3. Details of Mg#, MgO, FeO, F parameter, and % crystallization for each MI

30 minutes	Mg# (Fe2+)	MgO (wt%)	FeO (wt%)	F	% crystallized
	69.55	8.59	7.45	1.00	0.00
	69.50	8.30	7.21	1.00	0.07
	68.63	8.48	7.68	0.99	1.32
	68.52	8.68	7.90	0.99	1.48
	68.49	8.44	7.69	0.98	1.52
	68.48	8.48	7.97	0.98	1.54
	68.44	8.36	7.63	0.98	1.60
	68.33	8.47	7.94	0.98	1.75
	68.30	8.47	7.78	0.98	1.79
	68.29	8.16	7.50	0.98	1.80
	68.25	8.48	7.79	0.98	1.86
	68.08	7.87	8.21	0.98	2.11
	67.94	8.50	7.95	0.98	2.31
	67.86	8.16	7.66	0.98	2.43
	67.49	8.60	8.20	0.97	2.96
	67.30	7.97	7.53	0.97	3.23
	66.94	7.75	7.73	0.96	3.75
	66.81	8.54	7.79	0.96	3.94
	66.76	8.42	8.30	0.96	4.01
	66.52	7.95	7.66	0.96	4.36
	66.03	8.23	8.38	0.95	5.06
	65.96	8.30	8.48	0.95	5.16
	65.65	7.78	8.06	0.94	5.60
	65.52	7.90	7.72	0.94	5.79
	64.69	8.20	8.86	0.93	6.99
mean	**67.53**	**8.28**	**7.88**	**0.97**	**2.90**
2σ	**2.48**	**0.54**	**0.72**	**0.04**	**3.57**

4 days	Mg# (Fe2+)	MgO (wt%)	FeO (wt%)	F	% crystallized
	70.17	9.43	7.94	1.00	0.00
	69.85	9.45	8.08	1.00	0.46
	69.78	9.27	7.95	0.99	0.56
	69.62	9.39	8.11	0.99	0.78
	69.46	9.32	8.12	0.99	1.01
	69.19	8.98	7.92	0.99	1.39
	69.04	9.03	8.02	0.98	1.62
	68.83	9.03	8.10	0.98	1.92
	68.83	8.93	8.01	0.98	1.92
	68.76	8.98	8.08	0.98	2.01
	68.65	8.93	8.08	0.98	2.17
	68.52	8.93	8.13	0.98	2.35
	68.03	8.85	8.24	0.97	3.06
	66.01	8.67	8.84	0.94	5.93
	65.62	8.67	9.00	0.94	6.49
	64.65	8.73	9.45	0.92	7.87
	64.17	8.59	9.50	0.91	8.55
mean	**68.19**	**9.01**	**8.33**	**0.97**	**2.83**
2σ	**3.63**	**0.53**	**1.02**	**0.05**	**5.18**

1. Unpaired *t* test results CO_2 IN GLASS

P value and statistical significance:
The two-tailed P value equals 0.7011
By conventional criteria, this difference is considered to be not statistically significant.

Confidence interval:
The mean of 30 minutes minus 4 days equals 57.3646
95% confidence interval of this difference: From -242.3992 to 357.1284

Intermediate values used in calculations:
t = 0.3865
df = 41
standard error of difference = 148.432

Learn more:

GraphPad's web site includes portions of the manual for GraphPad Prism that can help you learn statistics. First, review the meaning of P values and confidence intervals . Then learn how to interpret results from an unpaired or paired *t* test. These links include GraphPad's popular *analysis checklists* .

Review your data:

Group	30 minutes	4 days
Mean	609.1415	551.7769
SD	338.2730	637.7026
SEM	65.1007	159.4256
N	27	16

2. Unpaired *t* test results H_2O IN GLASS

P value and statistical significance:
The two-tailed P value equals 0.0512
By conventional criteria, this difference is considered to be not quite statistically significant.

Confidence interval:
The mean of 30 minutes minus 4 days equals 0.00835
95% confidence interval of this difference: From -0.00005 to 0.01674

Intermediate values used in calculations:
t = 2.0085
df = 41
standard error of difference = 0.004

Learn more:

GraphPad's web site includes portions of the manual for GraphPad Prism that can help you learn statistics. First, review the meaning of P values and confidence intervals . Then learn how to interpret results from an unpaired or paired *t* test. These links include GraphPad's popular *analysis checklists* .

Review your data:

Group	30 minutes	4 days
Mean	0.01922	0.01088
SD	0.01555	0.00741
SEM	0.00299	0.00185
N	27	16

3. Unpaired *t* test results TOTAL CO_2

P value and statistical significance:
The two-tailed P value equals 0.1349
By conventional criteria, this difference is considered to be not statistically significant.

Confidence interval:
The mean of 30 minutes minus 4 days equals -460.97498
95% confidence interval of this difference: From -1071.36174 to 149.41178

Intermediate values used in calculations:
t = 1.5252
df = 41
standard error of difference = 302.240

Learn more:

GraphPad's web site includes portions of the manual for GraphPad Prism that can help you learn statistics. First, review the meaning of P values and confidence intervals . Then learn how to interpret results from an unpaired or paired *t* test. These links include GraphPad's popular *analysis checklists* .

Review your data:

Group	30 minutes	4 days
Mean	2253.06315	2714.03813
SD	800.17101	1182.65992
SEM	153.99298	295.66498
N	27	16

4. Unpaired *t* test results PRESSURES

P value and statistical significance:
The two-tailed P value equals 0.1293
By conventional criteria, this difference is considered to be not statistically significant.

Confidence interval:
The mean of 30 minutes minus 4 days equals -642.8940
95% confidence interval of this difference: From -1481.5353 to 195.7474

Intermediate values used in calculations:
t = 1.5482

df = 41
standard error of difference = 415.263

Learn more:

GraphPad's web site includes portions of the manual for GraphPad Prism that can help you learn statistics. First, review the meaning of P values and confidence intervals . Then learn how to interpret results from an unpaired or paired *t* test. These links include GraphPad's popular *analysis checklists* .

Review your data:

Group	30 minutes	4 days
Mean	4089.4685	4732.3625
SD	1184.1142	1518.2325
SEM	227.8829	379.5581
N	27	16

5. Unpaired *t* test results for %CO_2

P value and statistical significance:
The two-tailed P value equals 0.0064
By conventional criteria, this difference is considered to be very statistically significant.

Confidence interval:
The mean of 30 minutes minus 4 days equals -11.8188
95% confidence interval of this difference: From -20.1170 to -3.5206

Intermediate values used in calculations:
t = 2.8785
df = 40
standard error of difference = 4.106

Learn more:

GraphPad's web site includes portions of the manual for GraphPad Prism that can help you learn statistics. First, review the meaning of P values and confidence intervals . Then learn how to interpret results from an unpaired or paired *t* test. These links include GraphPad's popular *analysis checklists* .

Review your data:

Group	30 minutes	4 days
Mean	71.3052	83.1240
SD	14.1256	9.6898
SEM	2.7185	2.5019
N	27	15